Topological properties of the structural brain network constructed using the ε-neighbor method

Min-Hee Lee, Dong Youn Kim, Moo K. Chung*, Andrew L. Alexander and Richard J. Davidson

Abstract*— *Objective: **Structural characteristics of the brain can be analyzed based on structural brain networks constructed by diffusion tensor imaging (DTI). When a brain network is constructed by the existing parcellation method, the structure of the network changes depending on the scale of parcellation and arbitrary thresholding. To overcome these issues, we propose to construct brain networks using the improved ε-neighbor construction method, which is a parcellation free technique.** ***Methods:*** **We acquired DTI data from 14 control subjects and 15 subjects with autism. We examined the differences in topological properties of the brain networks constructed using the proposed method and existing parcellation between the two groups.** ***Results:*** **As the number of nodes increased, the connectedness of the network decreased in the parcellation method. However, for brain networks constructed using our proposed method, connectedness remained at a high level even with an increase in the number of nodes. We found significant differences in several topological properties of brain networks constructed using the proposed method, whereas topological properties were not significantly different for the parcellation method.** ***Conclusion:*** **The brain networks constructed using the proposed method are considered as more realistic than a parcellation method with respect to the stability of connectedness. We found that subjects with autism showed the abnormal characteristics in the brain networks. These results demonstrate that the proposed method may provide new insights to analysis in the structural brain network.** ***Significance:*** **We proposed the novel brain network construction method to overcome the shortcoming in the existing parcellation method.**

***Index Terms*—Autism, diffusion tensor imaging (DTI), ε-neighbor construction method, parcellation, structural brain network, topological properties.**

I. Introduction

THE human brain is a complex system capable of generating and integrating information from multiple sources in a highly efficient manner [1]. Defining the global architecture of the anatomical connection patterns of the human brain is important, because these connection patterns can provide new insights into correlations between functional brain disorders and underlying structural collapses [2], [3]. Diffusion tensor imaging (DTI) is a technique that facilitates non-invasive studies of the living human brain. Using DTI data, white matter tractography can determine the fiber bundle direction at each pixel and allow visualization of fiber bundles. The development of this technique has yielded large datasets of anatomical connection patterns [4]. Sporns *et al*. inferred the human brain connectome by using the DTI data, thus comprehensively describing the structure of element networks and connections forming the human brain [3]. Recently, attempts to model the human brain as a network of brain regions connected by anatomical tracts or functional associations have attracted considerable interest, because characterizing this structural and functional connectivity could impact studies of brain pathology and developmental disorders [5]. Comparisons of structural or functional network topological properties between subjects could reveal putative connectivity abnormalities in neurological and psychiatric disorders [4].

A network is set of nodes linked by edges. Nodes in a neural network correspond to individual neurons at the microscopic scale, but it is unclear how grey matter should be parcellated at the macroscopic scale [6]. In many studies, nodes are composed using the parcellation method [2], [6], [7], which is somewhat problematic in that the network structure is influenced by changes in both the parcellation scale and thresholding in connectivity matrices. Various topological parameters depend on the threshold level chosen. Because the topological properties of nodes changes according to parcellation scale, Zalesky *et al*. investigated how topological properties of the network, such as normalized path length, average normalized clustering coefficient, small-worldness, and node degree changed according to the parcellation scale used to divide brain regions. They argued that the parcellation scale should be carefully determined in structural brain network analysis [6].

To overcome these problems, Chung *et al*. proposed a network graph modeling technique called the ε-neighbor construction technique that does not use parcellation schemes [8]. The ε-neighbor method iteratively considers only two endpoints of each tract, designated as nodes on the graph, whereas tracts are designated as edges [8]. In this study, we

This research was supported by the Brain Research Program through the National Research Foundation of Korea (NRF) funded by the Ministry of Science, ICT & Future Planning (2016M3C7A1905385) and NIH Brain Initiative grant R01 EB022856. *Asterisk indicates corresponding author.*

M. H. Lee and D. Y. Kim are with the Department of Biomedical Engineering, Yonsei University.

A. L. Alexander and R. J. Davidson are with the Waisman Laboratory for Brain Imaging and Behavior, University of Wisconsin.

*M. K. Chung is with the Waisman Laboratory for Brain Imaging and Behavior, University of Wisconsin, Madison, WI 53706 USA (e-mail: mkchung@wisc.edu).

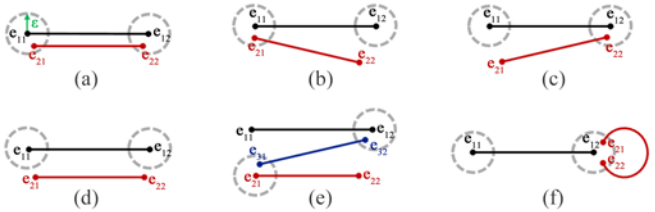

Fig. 1. Six possibilities of the ε-neighbor construction method: (a) e_{21} and e_{22} are all ε-neighbors of G_1. (b) Only e_{21} is an ε-neighbor of G_1. (c) Only e_{22} is an ε-neighbor of G_1. (d) Neither e_{21} nor e_{22} is an ε-neighbor of G_1. (e) e_{31} is an ε-neighbor of e_{21} in G_2 and e_{32} is an ε-neighbor of e_{12} in G_2. (f) e_{21} and e_{22} are ε-neighbors of e_{11} or e_{12} in G_1. This last relationship was considered to be noise, because it resulted in a circular tract.

improved the ε-neighbor construction method and evaluated the topological properties of structural brain networks constructed using both the parcellation method and our modified method.

Many neuropsychiatric disorders are considered to reflect abnormalities in brain connectivity [9]. Autism is a neurodevelopmental disorder characterized by impaired communication, social interaction, and social comprehension [10]. The increasing prevalence of autism has promoted interest in understanding brain functional and structural connectivity in this neurodevelopmental disorder [11]. Many studies have used functional magnetic resonance imaging (fMRI) to analyze and compare functional connectivity between control subjects and subjects with autism [12]-[15]. In studies comparing functional connectivity between these two groups, Cherkassky *et al*. observed lower connectivity in the left hemisphere of subjects with autism [13]. Belmonte *et al*. observed local functional over-connectivity and global functional under-connectivity in subjects with autism [12]. However, some studies reported that global under-connectivity was not always observed in subjects with autism, and concluded that observations of abnormal over-connectivity and under-connectivity require further experimental investigation [14], [15]. Other studies have used DTI data to analyze and compare structural connectivity between control subjects and subjects with autism [8], [9], [16], [17]. Chung *et al*. reported that the brain networks of subjects with autism exhibited slower integration rates than those of control subjects [8], and that subjects with autism had brain networks with more nodes with a low degree of connectivity than control subjects, thus demonstrating overconnectivity [17]. Using edge weight distribution, Adluru *et al*. also reported differences between control subjects and subjects with autism [16]. Dennis *et al*. reported that carriers of a common variant in the autism risk gene, CNTNAP2, had differences in structural connectivity. They found that subjects with autism had a shorter characteristic path length in the whole brain network, greater small-worldness, and greater global efficiency in the left hemisphere, and greater global efficiency in the right hemisphere [9]. Recently, Rudie *et al*. examined differences in topological properties in both structural and functional connectivity between control subjects and subjects with autism. They reported differences in topological properties of functional connectivity [18]. However, they did not observe differences in the topological properties of structural connectivity. To determine if there are differences in structural connectivity between the brain networks of control subjects and subjects with autism, we applied the improved ε-neighbor construction method to analyze and compare topological properties between brain networks derived from 14 control subjects and 15 subjects with autism.

II. Network Construction Methods

A. ε-neighbor Construction Method

In this section, we explain the ε-neighbor construction method in detail. Accepting the premise that the entire brain contains n tracts, the i-th tract will have two endpoints, e_{i1} and e_{i2}. In our network graph construction, we only considered the two endpoints of each tract. The endpoints of tract were considered to be nodes; tracts were considered to be edges in our graph. The 3-D graph is denoted as $G_k = \{V_k, E_k\}$ with node set V_k and edge set E_k at the k-th iteration of the ε-neighbor construction. The shortest Euclidean distance between point p of graph G_k and point q in V_k is defined as

$$d(p, G_k) = \min_{q \in V_k} \| p - q \| \tag{1}$$

Point p is designated an ε-neighbor of graph G_k if $d(p, G_k) \le \varepsilon$. Because ε is related to the scale at which the graph is constructed, ε is considered to be a measure of graph resolution. If ε has a large value, the constructed graph will have fewer nodes; in contrast, if ε has a small value, the constructed graph will have more nodes. Starting with two endpoints e_{11} and e_{12} of the first tract which has the longest length of tracts, the ε-neighbor construction method begins with graph G_1, with $V_1 = \{e_{11}, e_{12}\}$ and $E_1 = \{e_{11}e_{12}\}$. Next, the endpoints e_{21} and e_{22} from the second longest tract are added to the existing graph G_1. Note that the ε-neighbor construction method is performed in order from the longest tract to the shortest tract. Fig. 1 shows six possibilities of adding the second tract to graph G_1, as described below.

In Fig. 1(a), e_{21} and e_{22} are all ε-neighbors of G_1. Because the endpoints e_{21} and e_{22} are close to the existing graph G_1, node set V_1 and edge set E_1 do not change. Thus, $V_2 = V_1$ and $E_2 = E_1$.

In Fig. 1(b), only e_{21} is an ε-neighbor of G_1. Node e_{22} is added to node set V_1, and edge $e_{21}e_{22}$ is added to edge set E_1. Thus, $V_2 = V_1 \cup \{e_{22}\}$ and $E_2 = E_1 \cup \{e_{21}e_{22}\}$.

In Fig. 1(c), only e_{22} is an ε-neighbor of G_1. Node e_{21} is added to node set V_1, and edge $e_{21}e_{22}$ is added to edge set E_1. Thus, $V_2 = V_1 \cup \{e_{21}\}$ and $E_2 = E_1 \cup \{e_{21}e_{22}\}$.

In Fig. 1(d), neither e_{21} nor e_{22} is an ε-neighbor of G_1. Nodes e_{21}, e_{22} are added to node set V_1, and edge $e_{21}e_{22}$ is added to edge set E_1. Thus, $V_2 = V_1 \cup \{e_{21}, e_{22}\}$ and $E_2 = E_1 \cup \{e_{21}e_{22}\}$.

In Fig. 1(e), e_{31} is an ε-neighbor of e_{21} in G_2 and e_{32} is an ε-neighbor of e_{12} in G_2. The node set V_3 does not change; however, edge $e_{31}e_{32}$ is added to edge set E_2. Thus, $V_3 = V_2$ and $E_3 = E_2 \cup \{e_{31}e_{32}\}$.

In Fig. 1(f), e_{21} and e_{22} are ε-neighbors of either e_{11} or e_{12} in G_1. This relationship is considered to be noise since they result

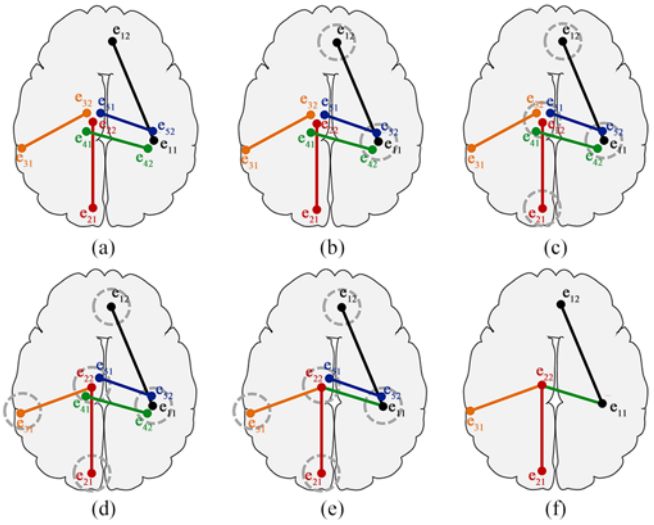

Fig. 2. Toy example of the network construction process using the ε-neighbor construction method. (a) Five sample tracts. (b) The ε-neighbor construction starts from graph G_1, which has $V_1 = \{e_{11}, e_{12}\}$ and $E_1 = \{e_{11}e_{12}\}$. (c) Neither e_{21} nor e_{22} is an ε-neighbor of G_1. Thus, $V_2 = V_1 \cup \{e_{21}, e_{22}\}$ and $E_2 = E_1 \cup \{e_{21}e_{22}\}$. (d) e_{32} is an ε-neighbor of G_2. Thus, $V_3 = V_2 \cup \{e_{31}\}$ and $E_3 = E_2 \cup \{e_{31}e_{32}\}$. (e) e_{41} is an ε-neighbor of e_{22} in G_3 and e_{42} is an ε-neighbor of e_{11} in G_3. Thus, $V_4 = V_3$ and $E_4 = E_3 \cup \{e_{41}e_{42}\}$. (f) e_{51} and e_{52} are all ε-neighbors of G_4. Thus, $V_5 = V_4$ and $E_5 = E_4$.

in a circular tract. Thus, $V_2 = V_1$ and $E_2 = E_1$. Previously in Chung *et al*., this case was simply ignored thus resulting in an additional noise in the network construction [8].

Fig. 2 shows a toy example for the ε-neighbor construction process. Fig. 2(a) represents five sample tracts, and the endpoints of the i-th tract are denoted by e_{i1} and e_{i2}. The ε-neighbor construction starts from graph G_1, which has $V_1 = \{e_{11}, e_{12}\}$ and $E_1 = \{e_{11}e_{12}\}$ as in Fig. 2(b). Next, the endpoints of the second longest tract (e_{21}, e_{22}) are used. Neither e_{21} nor e_{22} is an ε-neighbor of G_1. Thus, $V_2 = V_1 \cup \{e_{21}, e_{22}\}$ and $E_2 = E_1 \cup \{e_{21}e_{22}\}$ as in Fig. 2(c). In step 3, we use endpoints of the third longest tract (e_{31}, e_{32}). e_{32} is an ε-neighbor of G_2. Thus, $V_3 = V_2 \cup \{e_{31}\}$ and $E_3 = E_2 \cup \{e_{31}e_{32}\}$ as in Fig. 2(d). In step 4, we use the endpoints of the fourth longest tract (e_{41}, e_{42}). e_{41} is an ε-neighbor of e_{22} in G_3 and e_{42} is an ε-neighbor of e_{11} in G_3. Thus, $V_4 = V_3$ and $E_4 = E_3 \cup \{e_{41}e_{42}\}$ as in Fig. 2(e). Finally, we use the endpoints of the last longest tract (e_{51}, e_{52}). e_{51} and e_{52} are all ε-neighbors of G_4. Thus, $V_5 = V_4$ and $E_5 = E_4$ as in Fig. 2(f).

We constructed brain networks using the ε-neighbor construction method as shown in Fig. 3(a). The resulting 3D graph for a network can be parameterized by transforming the existing graph to an adjacency matrix. The adjacency matrix $A = (adj_{ij})$ of a graph is constructed by adding new edges to the existing edge set. If nodes i and j are connected, $adj_{ij} = 1$. Otherwise, $adj_{ij} = 0$. The adjacency matrix is symmetric and contains sufficient information to reconstruct the graph. The adjacency matrix is also an important parameter for analyzing the topological properties of the network.

B. *Parcellation Method*

We also constructed the brain network using the parcellation method for comparison against the proposed method. To construct a network graph using the parcellation method, we used the automated anatomical labeling (AAL) template [19]. The standard AAL template parcellates the brain into 116 regions, which form the nodes of the brain network. Let $P(i)$ denote the i-th node. Let S and E be the endpoints of each tract. Adjacency matrix $A = (adj_{ij})$ was defined as

$$adj_{ij} = \sum I_{\{S \in P(i)\}} I_{\{E \in P(j)\}} + I_{\{S \in P(j)\}} I_{\{E \in P(i)\}}, \quad (2)$$

where if the endpoint S lies at the i-th node $P(i)$, $I_{\{S \in P(i)\}} = 1$, otherwise $I_{\{S \in P(i)\}} = 0$ [6]. Because some topological properties of weighted graphs are ill-defined [6], we only considered binary graphs. We binarized graphs by assigning one to all non-zero entries for each adjacency matrix. The result of network construction using the parcellation method and its adjacency matrix are shown in Fig. 3(b).

III. Network Analysis Methods

Complex networks have received recent attention from a range of disciplines, including social science, information science, biology, and physics [1]. Numerous studies have analyzed networks according to their topological properties [2], [6], [20], [21]. Complex network analysis is an approach that characterizes datasets and describes the properties of complex systems by quantifying the topologies of the associated networks. Complex network analysis is based on graph theory, a mathematical approach for studying networks [4]. In this study, we used the topological properties such as path length, global efficiency (E_{glob}), clustering coefficient, local efficiency (E_{loc}) node degree, density, node betweenness centrality (NBC), and regional efficiency (E_{reg}) to analyze structural brain networks.

A. *Path Length*

In the brain, functional integration is the ability to combine information from multiple brain regions. A measure of this integration is often based on the concept of path length. Path length measures the ability to integrate information flow and functional proximity between pairs of brain regions [1], [4]. When the path length becomes shorter, the potential for functional integration increases [1]. Path length in undirected binary network is equal to the number of edges in the path [1].

B. *Clustering Coefficient*

Clustering coefficient describes the ability for functional segregation and efficiency of local information transfer. Clustering coefficient for node i is calculated as the number of existing connections between the neighbors of node i divided by the number of all possible connections [22]. Typically, clustering coefficient C has been calculated as the average clustering coefficient over all the nodes.

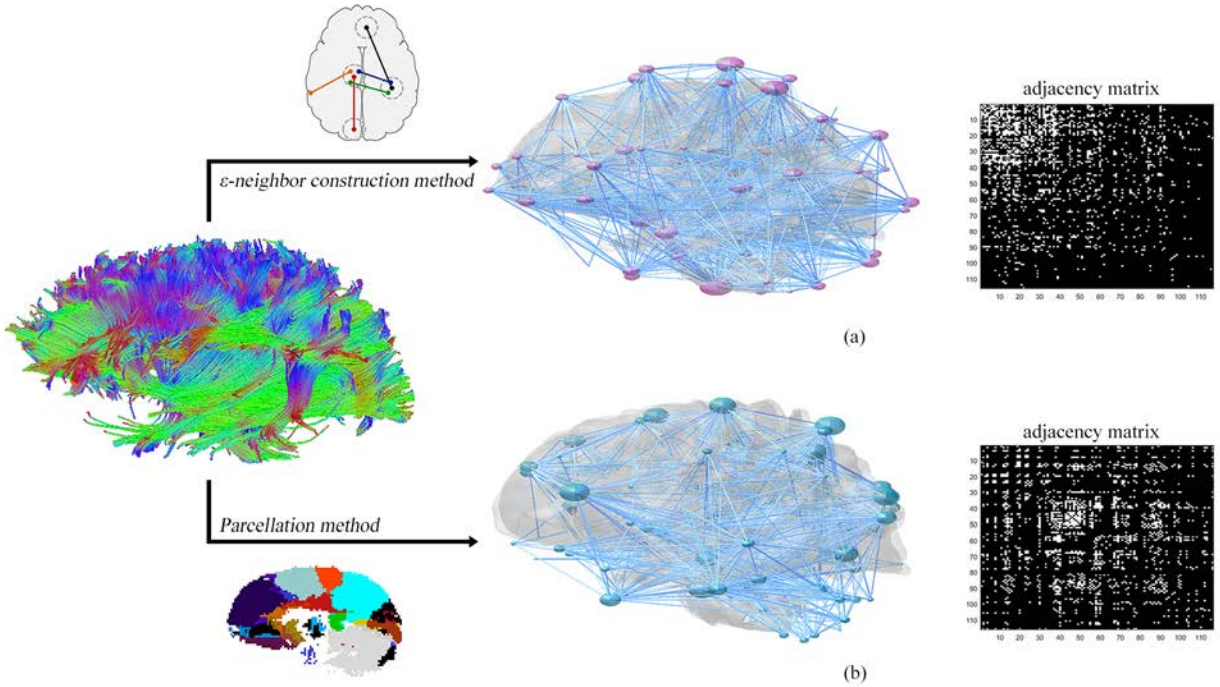

Fig. 3. Example of constructed brain network. (a) Structural brain network constructed by the ε-neighbor construction method. Nodes are located in the center of ε sphere. (b) Structural brain network constructed by the parcellation method. Nodes are located in the center of gravity of each AAL region.

C. Small-World

The small-world method of network analysis, with clustering coefficient C_p and average path length L_p, was proposed by Watts and Strogatz [22]. A real network was considered to be a small-world network if it met the following criteria:

$$\gamma = C_p^{real} / C_p^{rand} >> 1$$
$$\lambda = L_p^{real} / L_p^{rand} \approx 1 \quad (3)$$
$$\sigma = \gamma / \lambda > 1$$

where C_p^{real} and L_p^{real} are the average clustering coefficient and characteristic path length of real network. C_p^{rand} and L_p^{rand} are the average clustering coefficient and characteristic path length of random networks that preserved the number of nodes, edges, and node degree distributions present in the real network. In our experiment, we used 100 random networks for each real network. Recent studies have demonstrated that human brain networks derived from DTI have small-world properties [2], [6], [23]. Small-world networks have high clustering coefficients and short path lengths and might provide the underlying structural substrates of functional integration and segregation in the human brain [2].

D. Network Efficiency

E_{glob} is defined as the average of the inverse of the shortest path length between nodes [24]. The E_{glob} of a brain network refers to the efficiency of parallel information transfer in the network [24]. E_{glob} reflects integration over the whole brain network [25].

The E_{loc} measures the fault-tolerance of the network and ability of information exchange in sub-network [26]. This measure is defined as the efficiency of the connections between the nearest neighborhoods of the node [24].

To determine the regional characteristics of the brain network, we computed E_{reg} in this study. E_{reg} measures the average path length between given node i and the remaining nodes in a network [7], and reflects the integration of each node [25]. The E_{reg} of a brain network can be defined as follows:

$$E_{reg}(i) = \frac{1}{n-1}\sum_{i \neq j}\frac{1}{d_{ij}}, \quad (4)$$

where d_{ij} is the shortest path length between nodes i and j and n is the total number of nodes.

E. Node Degree

Node degree in a graph is defined as the numbers of connections with other nodes. Typically, node degree is calculated as the average for all the nodes. A node with a high degree is interacting, structurally or functionally, with many other nodes in the network [4].

Node degree distribution shows resilience to targeted attack, i.e., node removal [27], [28]. Human brain network has previously been considered to be a scale-free network, implying the existence of a few highly connected nodes with superior resilience to random node failures [1], [29]. Recently, studies have claimed that the human brain network is not a scale-free network [2], [6], [20]. To test for scale-freeness, we fitted node degree distribution to three distinct models as follows:

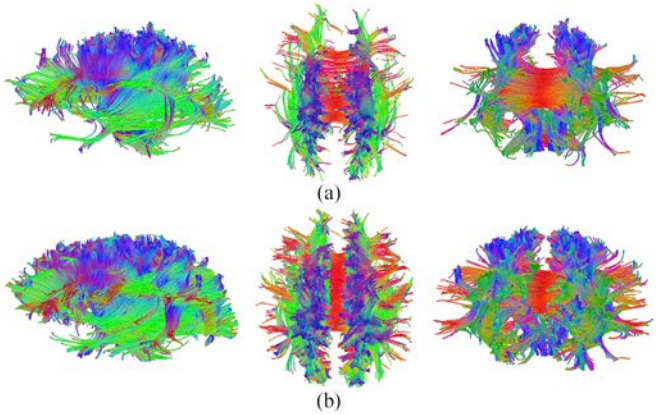

Fig. 4. The results of culling tracts. A tract was considered usable if it intersected one of the parcellations in the AAL template. Tracts with a tract length less than 10 mm were also culled as these were considered to be noise tracts. Also tracts that do not connect any two AAL parcellations are culled. (a) Culled tracts. (b) Usable tracts.

$$\begin{aligned} &\text{power law}: x^{(\alpha-1)} \\ &\text{exponential}: e^{(-x/x_c)} \\ &\text{exponentially truncated power law}: x^{(\alpha-1)}e^{(-x/x_c)} \end{aligned} \tag{5}$$

where x is the node degree value, x_c denotes estimated cutoff degree, and α is the estimated exponent. Node degree distribution was fitted using the curve fitting toolbox of MATLAB and goodness of fit was assessed by R-squared values.

F. Density

Network density is a measure of the number of connections compared to the maximum possible number of connections between nodes, and indicates how well the network is connected [30]. Biological networks, however, are characterized by a small number of connections compared to all possible connections [30]. Low densities describe sparse graphs, whereas high densities describe dense graphs. However, the appropriate criteria to use for discriminating between sparse and dense graphs are ambiguous [31].

G. Connected Component

A connected component is a sub-graph whose nodes are connected by edges. The number of connected components of the graph is the number of structurally independent or disconnected sub-graphs that can be measured from its topological properties. To identify connected components, we used the Dulmage-Mendelsohn decomposition method, a method widely used for decomposing a sparse matrix [32]. The largest connected component was defined as the connected component with the largest number of nodes [33].

Network connectedness refers to how well network nodes are connected. Let N be the number of nodes in the network. If the size of the largest connected component approaches N, the connectedness will increase [34]. In this study, we calculated the size of the largest connected component as a proportion of N.

H. Node Betweenness Centrality

In a complex network, node betweenness centrality (NBC) can be used to determine the relative importance of a node and to represent the communication load. NBC can measure the influence of a node over information flow between other nodes in the network [2]. The betweenness centrality of a given node v is defined as

$$NBC = \sum_{i \neq V \neq j} \frac{\sigma_{ij}(v)}{\sigma_{ij}} \tag{6}$$

where σ_{ij} is the number of shortest paths between nodes i and j and $\sigma_{ij}(v)$ is the number of shortest paths passing through node v [35], [36].

To gain a deeper understanding of the connection structure of our networks, we performed node attacks [27], [28]. Then, to observe the effects of removing nodes on the network, we calculated the size of largest connected component after removal of a node. Node attacks were performed as follows:

a) For random node attack, we removed randomly chosen nodes of the structural brain network until the size of largest connected component becomes zero and repeated this procedure 1000 times.
b) For the targeted node attack, we employed NBC in multiple previous studies to define the node for targeted attack [27], [28]. We removed the nodes in decreasing order of their NBC. The removal process continues until the size of largest connected component becomes zero.

We compared the size of largest connected component between two groups for each removal step.

I. Statistical Analysis

Matlab version R2014a (Mathworks, Natick, MA, USA) was used to analyze the topological properties of the brain networks and statistical analysis. In this study, we used a nonparametric permutation t-test for the statistical analysis in all network properties between control subjects and subjects with autism [37]. Briefly, we computed the two-sample t-statistic between p-value the two groups and then we randomly permuted the group labels. Finally, we recomputed t-statistics between the permuted groups.

In this study, the permutation was repeated 10000 times. We determined the 95 percentile points of each t-statistics distribution as a critical value (p-value = 0.05). The p-values were adjusted for multiple comparisons using the false discovery rate (FDR) correction.

TABLE I
CONNECTEDNESS COMPARISON BETWEEN THE PARCELLATION AND ε-NEIGHBOR CONSTRUCTION METHODS

	Parcellation Method		ε-neighbor Construction Method	
	Mean	SD	Mean	SD
116 Nodes	0.906	0.025	0.999	0.006
221 Nodes	0.935	0.024	0.999	0.003
330 Nodes	0.887	0.032	0.997	0.004
456 Nodes	0.820	0.033	0.994	0.005
561 Nodes	0.786	0.032	0.993	0.005

SD: standard deviation.

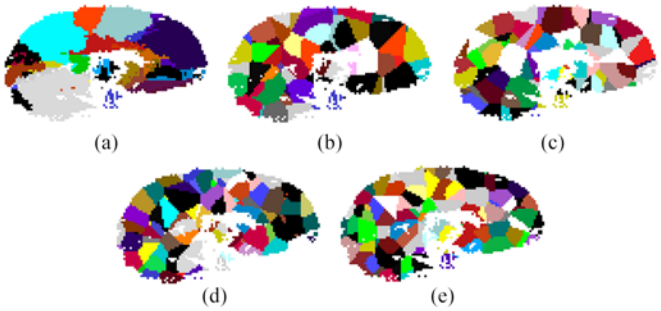

Fig. 5. Results of additional parcellation. To observe how topological properties of the network changed according to the number of nodes, we parcellated additional subregions within AAL parcellations. (a) 116 nodes (b) 221 nodes (c) 330 nodes (d) 456 nodes (e) 561 nodes.

IV. CLINICAL APPLICATION

A. Data Acquisition and Pre-processing

We analyzed DTI data from a total of 29 subjects, comprising 14 control subjects (*12.1* ± *2.7* years old, range *10* - *19*) and 15 subjects with autism (*13.9* ± *3.3* years old, range *10* - *22*) who were matched for age, handedness, IQ, and head size.

To acquire DTI with more directions, scans take more time and children with autism may have difficulty staying still [38]. In addition, Yendiki *et al*. reported that children with autism showed more head motion than typically developing children [39]. The longer scan time causes more head motion and we may acquire incorrect DTI parameters [39]. Thus, DTI data were obtained for a single (b = 0) reference image and 12 non-collinear diffusion-encoding directions, with a diffusion weighting factor of b = 1000 s/mm^2.

Distortion associated with eddy currents and head motion for each dataset was adjusted using automated image registration (AIR) [40]. Distortions from field inhomogeneities were adjusted using custom software algorithms [41]. The six tensor elements were calculated using non-linear fitting methods [42]. We used nonlinear tensor image registration algorithms for spatial normalization of DTI data [43], and performed streamline-based tractography using the TENsor Deflection (TEND) algorithm [44], [45].

B. Comparison of Topological Properties according to Network Construction Method

In this study, we proposed a novel brain network construction method that does not involve parcellation scheme. To evaluate the proposed method, we compared the topological properties of brain networks constructed using our method and those constructed from the conventional parcellation method. To construct two network graphs for each subject (i.e., 58 network graphs for 29 subjects), image processing steps such as template normalization, culling tracts, and matching of the number of nodes were required. We also performed the template normalization due to differences between templates. We performed 3D non-linear image registration between fractional anisotropy and AAL templates using Ezys [46]. This enabled us to use both methods in a normalized space. Next, a tract was considered usable if each endpoint of the tract intersected one of the parcellations in the AAL template. Unusable tracts were culled from the set of all tracts. Moreover, tracts that were less than 10 mm in length were also culled because they were considered to be noise tracts. Culling is a necessary step to eliminate spurious tracts that do not interconnect in the parcellation method [6].

During this processing step, we found that there are many unusable tracts in one subject, which is considered as an outlier. For this reason, we used 56 network graphs for 28 subjects in this comparison after removing one outlying subject. After culling tracts, we used the same usable tracts in both methods. Our DTI data had *3056.7* ± *266.21* culled tracts and *6943.30* ± *266.21* usable tracts (see Fig. 4). Finally, to determine how topological properties of the network changed according to the number of nodes in both methods, we adjusted the ε-radius in the ε-neighbor construction method and parcellated additional subregions within AAL using the algorithm proposed by Zalesky (see Fig. 5) [6]. This results in networks with 116, 221, 330, 456, and 561 nodes.

V. RESULTS

A. Differences in Topological Properties according to Network Construction Method

We analyzed network structures in terms of connectedness as a function of the parcellation scale and ε-radius. The change in connectedness according to parcellation scale and ε-radius are summarized in Table I. As the number of nodes increased, connectedness decreased for the parcellation method. However, connectedness was almost always one when the ε-neighbor construction method was used. Therefore, we chose parcellation scales with less than 10% disconnectedness (i.e., 116 nodes and 221 nodes) to compare topological properties of the brain networks constructed using the two methods. For the ε-neighbor construction method, at 116 nodes, subjects with autism exhibited a significantly higher E_{glob} (t-stat. = -1.6918, p-value = 0.0496) and node degree (t-stat. = -1.9581, p-value = 0.0323). However, subjects with autism showed no significant differences (corrected p-value < 0.05). For the parcellation method, we could not observe the differences in global properties between the two groups. At 221 nodes, the brain networks of subjects with autism exhibited a significantly higher E_{glob} (t-stat. = -2.8104, p-value = 0.0053) and density (t-stat. = -2.5161, p-value = 0.0097) than those of control subjects in only the ε-neighbor construction method (Table II).

TABLE II
DIFFERENCES IN GLOBAL PROPERTIES BETWEEN CONTROL SUBJECTS AND SUBJECTS WITH AUTISM FOR THE ε-NEIGHBOR CONSTRUCTION METHODS

		Control		Autism		Group Differences		
		Mean	SD	Mean	SD	t-statistics	p-value	Corrected p-value
116 Nodes	Global Efficiency	0.471	0.013	0.478	0.011	-1.692	0.050*	0.072
	Local Efficiency	0.538	0.032	0.546	0.027	-0.754	0.237	0.237
	Density	0.106	0.008	0.110	0.007	-1.678	0.054	0.072
	Degree	12.173	0.605	12.739	0.880	-1.958	0.032*	0.072
221 Nodes	Global Efficiency	0.391	0.006	0.398	0.007	-2.810	0.005**	0.020*
	Local Efficiency	0.362	0.018	0.361	0.031	0.148	0.442	0.442
	Density	0.046	0.002	0.049	0.004	-2.516	0.010**	0.020*
	Degree	10.338	0.203	10.531	0.407	-1.530	0.068	0.091

SD: standard deviation; *: Significant at the 0.05 level; **: Significant at the 0.01 level.

TABLE III
GROUP DIFFERENCES IN AREA UNDER CURVE OF GLOBAL PROPERTIES

	Control		Autism		Group Differences		
	Mean	SD	Mean	SD	t-statistics	p-value	Corrected p-value
Path length	12.351	0.165	12.191	0.163	2.582	0.008**	0.040*
Global efficiency	2.301	0.030	2.328	0.034	-2.232	0.017*	0.040*
Clustering coefficient	1.772	0.083	1.809	0.1028	-1.052	0.154	0.180
Local efficiency	2.631	0.090	2.686	0.125	-1.338	0.102	0.143
Small-worldness	6.421	0.274	6.374	0.313	0.405	0.348	0.348
Density	0.482	0.018	0.496	0.025	-1.722	0.049*	0.086
Degree	67.912	1.932	70.410	3.332	-2.465	0.012*	0.040*

SD: standard deviation; *: Significant at the 0.05 level; **: Significant at the 0.01 level.

B. *Abnormalities of Topological Properties in Autism Subjects*

1) Global Properties: Since each endpoint of tracts is assigned to one of the nodes in the proposed method, we did not undergo the culling process for our brain network analysis. To avoid the biased results owing to selection of a specific ε-radius, we had chosen a range of the graph resolution ε-radius (7~12mm) with the following conditions:

a) The number of nodes are more than 90 nodes (when ε-radius becomes 12 mm) which is frequently used as network scale in previous brain network studies [7], [25], [48] and fewer than 500 nodes (when ε-radius becomes 7 mm) which is often the highest number of nodes used in brain network analysis.
b) The number of nodes and edges between two groups are similar to each other.

For comparison of global properties between the two groups, we computed the area under curve (AUC) for each global property.

We first evaluated whether the brain networks constructed using the proposed method were small-world networks. In this study, since all subjects met the small-worldness criteria for a range of ε-radius, the constructed brain networks can be considered to be small-world networks (see Fig. 6). Moreover, we could not observe significant differences in small-worldness between the two groups. Small-world networks can be classified into three categories - power law, exponential, and exponentially truncated power law - according to their degree distributions [47]. We observed the node degree distribution in our constructed brain network and found that node degree distributions fit well to an exponentially truncated power law in both control subjects and subjects with autism, as shown in Fig. 7. The better fit of the data to the exponentially truncated power law distribution model indicated that the brain networks had some hub nodes and bridge edges, whereas large hub nodes or bridge edges with high loads were absent from the networks [2]. The small-worldness and node degree distribution of our constructed brain network are in agreement with prior studies [2], [6].

We next evaluated if there were abnormalities in the brain networks of subjects with autism. For this, we compared global topological properties of the brain network, including path length, clustering coefficient, E_{glob}, E_{loc}, node degree, and density, between the two groups. In the global properties, subjects with autism exhibited a significantly shorter average path length (t-stat. = 2.5823, p-value = 0.0075), higher E_{glob} (t-stat. = -2.2315, p-value = 0.0169), and higher degree (t-stat. = -2.4648, p-value = 0.0119) at corrected p-values < 0.05. However, we could not observe differences in density, clustering coefficient and E_{loc} between the two groups. Global properties for the brain network of each subject, including means, standard deviations of AUC, and results of group comparisons using non-parametric permutation t-test, are summarized in Table III and Fig. 8.

2) The Effects of Node Attack in the Brain Network: To examine the effects of node attack in the network, the brain networks were constructed at the ε-radius of 7mm. This

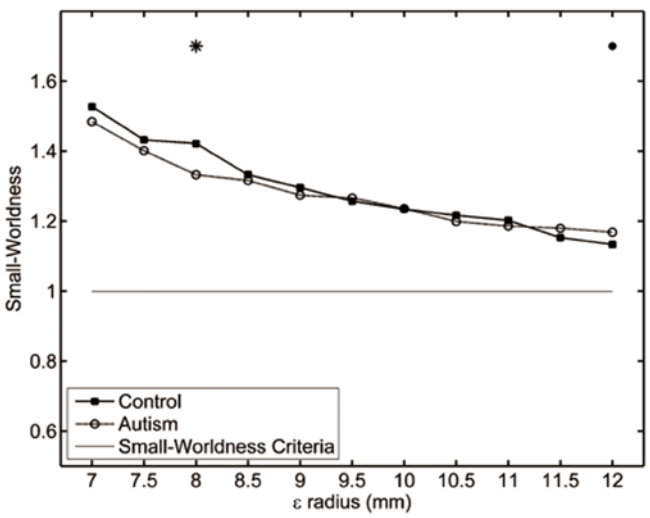

Fig. 6. Assessment of small-worldness as a function of ε radius in the structural brain network of control subjects and subjects with autism. Control subjects and subjects with autism met the small-worldness criteria for all ε radius. There was no significant difference in the area under curve of small-worldness between the two groups.

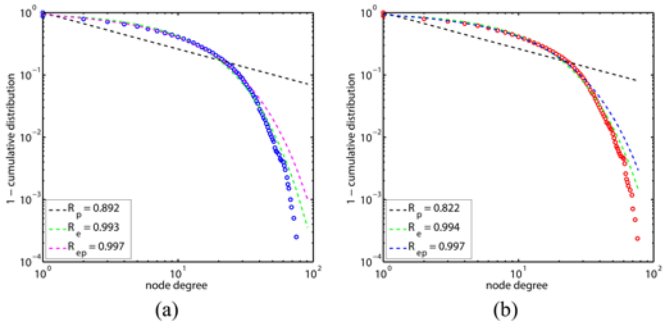

Fig. 7. Degree distribution of the brain network. The three models (power law: $x^{(\alpha-1)}$, exponential: e^{-x/x_c}, and exponentially truncated power law: $x^{(\alpha-1)}e^{-x/x_c}$ were fitted. R-square was calculated to determine the good of fit (R-square for the power law (R_p), for the exponential (R_e), and exponentially truncated power law (R_{ep})). (a) For the three models exponentially truncated power law model yielded the best fit for the brain network in control subjects (exponent $\alpha = 0.9148$, cutoff degree $x_c = 13.96$, $R_{ep} = 0.997$). (b) For the three models exponentially truncated power law model yielded the best fit for the brain network in subjects with autism (exponent $\alpha = 0.925$, cutoff degree $x_c = 14$, $R_{ep} = 0.997$).

resolution is the smallest integer that satisfied the following conditions:

a) Graph resolution produced fewer than 500 nodes to reduce computational complexity.
b) The values of many network measures are influenced by the number of nodes and edges [4]. Therefore, we chose the graph resolution such that outliers or significant differences in the numbers of nodes and edges between control subjects and subjects with autism did not exist.

At this resolution, we performed random and targeted node attack based on NBC. In this study, brain networks were more vulnerable to targeted node attack than random node attack and it is consistent with prior studies [27], [48]. Furthermore, we could not detect statistical difference in the size of largest connected component for the random attack. However, we observed that subjects with autism are more tolerant than control subjects for targeted node attack based on NBC across 9 to 33 of removed nodes (p-value < 0.05) (Fig. 9).

3) Regional Efficiency: We also investigated if there were alterations in the regional characteristic of the whole brain networks of subjects with autism. To do this, we compared E_{reg} for each region between control subjects and subjects with autism. The E_{reg} was also calculated at the specific resolution (ε-radius of 7mm). Since the locations of nodes are different among subjects, we averaged the E_{reg} of the nodes that lie in the same AAL region. In the comparisons of E_{reg}, we observed increased E_{reg} in the right superior temporal gyrus (t-stat. = -2.3964, p-value = 0.01) and left middle temporal gyrus (t-stat. = -2.2982, p-value = 0.0104) in subjects with autism relative to control subjects (Fig. 10). However, subjects with autism showed no significant differences in E_{reg} (corrected p-value < 0.05).

VI. Validation Against Existing Method

We performed the validation for similarity between networks constructed using the ε-neighbor construction method and the parcellation method. Since location and the number of nodes in the networks constructed using the proposed method may be different from networks constructed using the parcellation method, we transformed the networks constructed using our method to parcellation scheme. Firstly, we obtained the locations of nodes in the networks constructed using our method. Second, we combined the nodes located in a volume of AAL template into one node. For example, if nodes 1 and 2 are located in the volume 1 in AAL template, three nodes are combined into node 1 in the parcellation scheme (Fig. 11(a)). Finally, we calculated correlation coefficient using the Spearman rank correlation between the networks constructed using two methods to determine the similarity.

In this analysis, we observed that the network with the larger ε-radius showed lower correlation compared to the network constructed using the parcellation method (Fig. 11(b)). It is likely that ε-ball with large ε-radius includes multiple nodes in AAL template (Fig. 11(c)). For this reason, the correlation with the parcellation method became smaller as the ε-radius becomes large. Several studies used templates other than AAL template [49] or study specific templates [50].

VII. Evaluating the Sensitivity of the Scheme to the Order in Which Streamlines are Processed

To investigate the sensitivity of the order in which streamlines are processed, we have randomly ordered tracts and applied the same procedure. Since the brain network constructed by randomly ordered tracts may produce different results, we generated 900, 1000 and 1100 brain networks constructed by randomly ordered tracts. Then, we compared the topological properties including density, connectedness, path

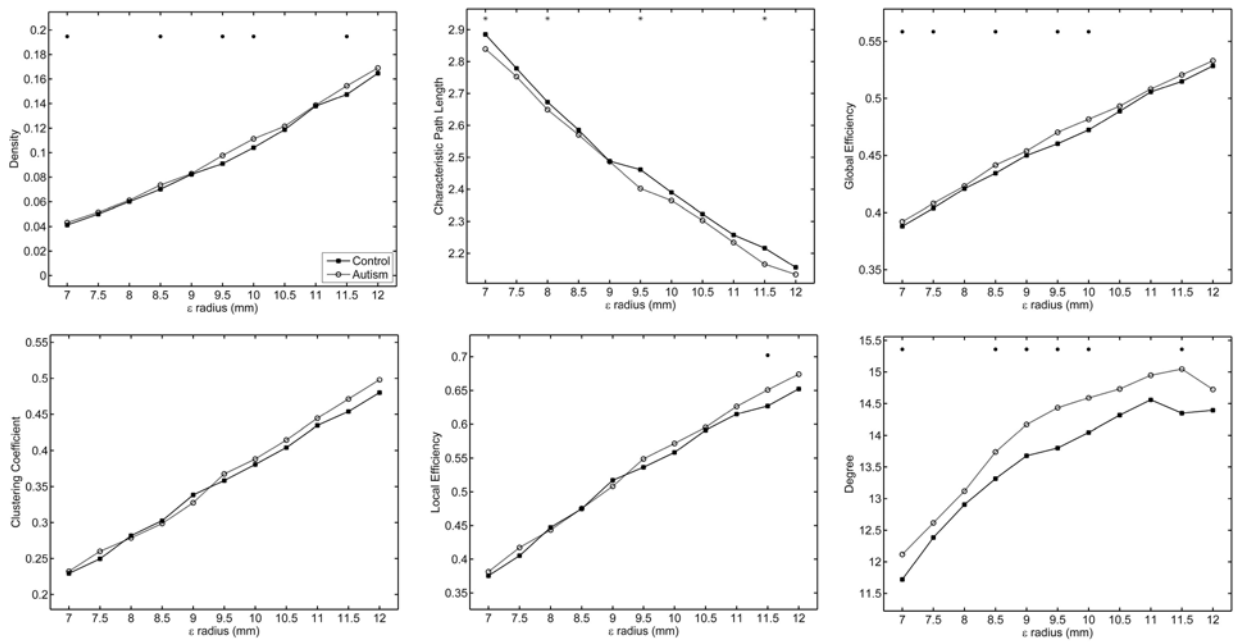

Fig. 8. Comparisons of topological properties between control subjects and subjects with autism. For statistical analysis, area under curve was calculated for each global property. Asterisk (*) means that control subjects have higher value of topological property than subjects with autism at a given ε radius ($p < 0.05$). Dot (.) means that subjects with autism have lower value of topological property than control subjects at a given ε radius ($p < 0.05$). We observed significant differences in area under curve of density, characteristic path length, global efficiency, and degree between two groups.

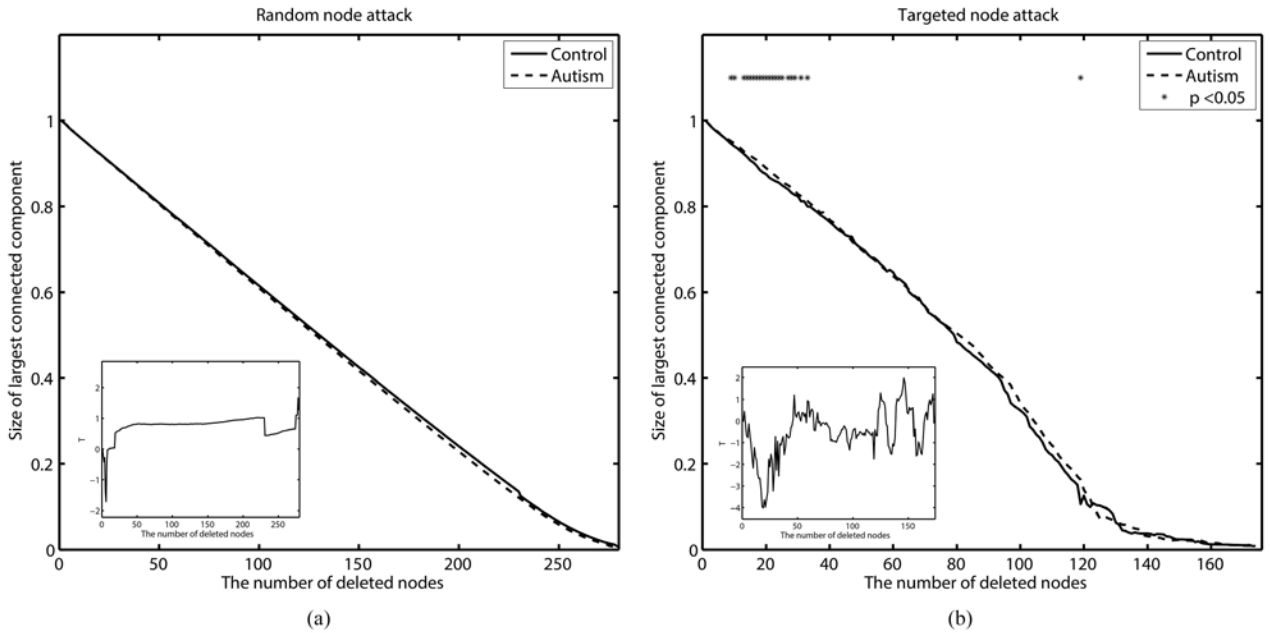

Fig. 9. Changes in the size of largest connected components for node attacks. (a) The change in size of largest connected component over the number of deleted nodes during the node attack. We could not observe the difference in the sizes between the two groups. (b) The change in size of largest connected component during the targeted node attack. We observed significant differences in the sizes between the two groups. The asterisk indicates that subjects with autism have higher size of largest connected component than control subjects at a given removal step ($p < 0.05$).

length, clustering coefficient, global efficiency, local efficiency and degree between the brain networks processed in the order of tract length and random order of tract. Before the comparison of topological properties, we examined whether there are differences in the number of nodes and edges. Since the number of nodes and edges greatly influences topological properties [4], this procedure is needed to compare the network properties on the same network scale (i.e., same number of nodes and edges).

We found that the brain networks constructed by the randomly ordered tracts have smaller number of nodes and edges than the brain networks constructed by the ordered length of tracts on the same ε-radius range (7:0.5:12). For fair comparisons, it was necessary to compare networks with the same number of nodes and edges. Therefore, we used the ε-radius range (6.8:0.5:11.8) for the network constructed by randomly ordered tracts. No significant differences in the number of nodes and edges were

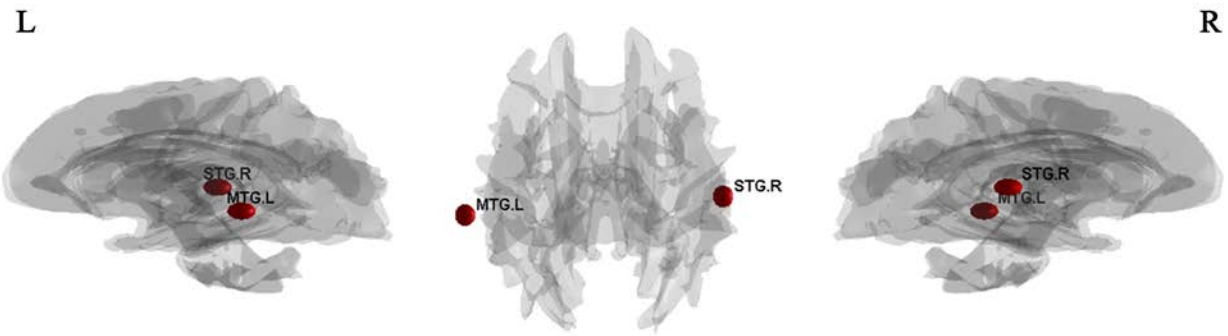

Fig. 10. Nodes disrupted in subjects with autism. Nodes with a regional efficiency higher in subjects with autism than control subjects are shown in red spheres ($p < 0.05$). No regions showed lower regional efficiency in subjects with autism. STG.R, right superior temporal gyrus; MTG.L, left middle temporal gyrus.

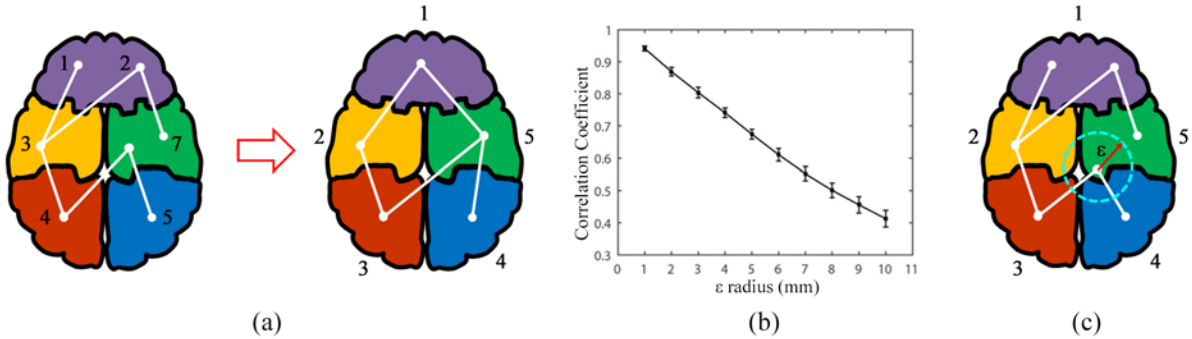

Fig. 11. Validation against existing method. (a) Combination of the nodes located in a volume of AAL template into one node. (b) The correlation coefficient between the brain networks constructed using two methods. (c) A node with large ε radius including multiple volume in AAL template.

found between the brain networks constructed by the ordered length of tract (ε-radius range = 7:0.5:12) and randomly ordered tracts (ε-radius range = 6.8:0.5:11.8) for 900, 1000, and 1100 brain networks. In addition, we could not find the differences in topological properties between the brain networks constructed by the ordered length of tracts and randomly ordered tracts on the same network scales.

The advantages of using the ordered length of tracts over randomly ordered length are as follows.

1) Construction of 1000 brain networks using randomly ordered tracts took approximately 90 hours for parallel computation using on a quad-core machine. However, construction of brain networks using the ordered length of tracts method took approximately 5 minutes on the same system.
2) The brain networks constructed by the ordered length of tracts and the random order have similar topological properties on the same network scales. The ordering of tracts do not effect significantly on the overall topological properties.
3) Nodes' locations between subjects are similar at a given ε-radius in the brain networks constructed by the ordered length of tracts method.

For these reasons, we consider that the construction of brain network using the ordered length is appropriate.

VIII. Simulating the Null Data Between Control and Autism Groups Through Split-Half Experiment

Since it is difficult to obtain real data with the ground truth, we performed a simulation study. We combined 14 control subjects and 15 subjects with autism and randomly split them evenly so that Group I has 7 control subjects and 7 subjects with autism while Group II has 7 control subjects and 8 subjects with autism. It is expected that there is no group difference between Group I and Group II. This process is repeated 10000 times to ensure that the desired error rate is controlled. We did not detect the difference in topological properties between the randomly split groups (all p-values ≥ 0.4). This controlled experiment shows that our method is not producing false positives in the null data.

IX. Other Type of ε-Neighbor Construction Method

Our proposed method is a static approach. We also considered a dynamic approach, where we adjusted the center of ε-balls at each iteration. We adjusted the coordinates of ε-ball centers (i.e., coordinates of previous node) when a new endpoint was merged to the existing endpoint. The coordinates of the existing node e_1 are adjusted to e'_1 as

$$e_1' = \frac{e_1 + \sum_{k=1}^{n} e_{1k}}{n+1}, \tag{7}$$

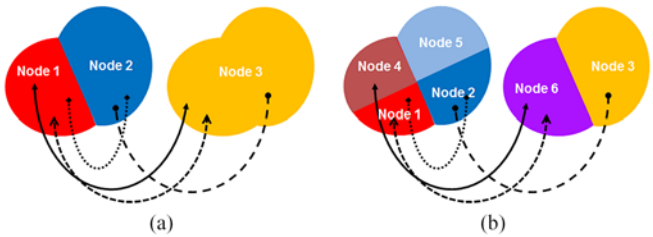

Fig. 12. Example of decreased connectedness using the parcellation method. When the parcellation scales are reduced, the number of nodes not intersected by any tracts increases. (a) All nodes are intersected by tracts. (b) Node 5 is not intersected by any tract. Connectedness decreases in the parcellation method as the parcellation scale becomes finer.

where e_{1k} is the coordinates of the k-th node that is merged to the existing node and n is the total number of nodes that are merged. The next step of network construction was proceeded based on the ε-ball with new center coordinates. We compared topological properties between the brain networks constructed by the static and dynamic ε-neighbor construction methods. The brain networks constructed by the static ε-neighbor construction method had significantly more nodes (p-value < 0.05) at all ε-radius range (7:0.5:12) and significantly fewer edges (p-value < 0.05) at some ε-radius range (10:0.5:12) than the dynamic method. In addition, the brain networks constructed by the static method showed significant differences in topological properties compared to the brain networks constructed by the dynamic method (p-value < 0.05). Unlike the static method, we could not observe significant differences in topological properties between the control subjects and the subjects with autism in the brain networks constructed by the dynamic method.

The endpoints of fiber tract that are inside ε-radius in the static method may be outside ε-radius in the dynamic method due to the adjusted ε-ball center. On the other hand, the endpoints that are outside ε-radius in the static method may be inside ε-radius in the dynamic method. For these reasons, approximately 38% of all nodes in the brain networks constructed by the dynamic method originated from the different tracts compared to the nodes constructed by the static method. It implies that the brain networks constructed by the dynamic method have a different organization compared to the networks constructed by the static method. The topological properties obtained by the dynamic method are different from the topological properties obtained by the static method.

In addition, we compared the similarity between brain networks constructed using the static ε-neighbor and the parcellation methods, the dynamic ε-neighbor and the parcellation methods that followed the procedure described in section VI. The correlation between statistic and parcellation methods is higher than that between the dynamic and parcellaiton methods (t-stat. = 2.161, p-value = 0.018). High correlation with the parcellation method implies that the network is similar to the parcellation method. Since parcellation method is based on anatomical brain regions, the static method is a more meaningful method than the dynamic method.

Further research is needed into the comparisons of the static and dynamic ε-neighbor construction methods from various datasets.

X. Discussion

The human brain can be modeled as a network. Analyzing brain networks could reveal abnormal connectivity in neurological and psychiatric disorders. Structural brain networks are sets of nodes (brain regions) linked by edges (anatomical tracts). Nodes composing the brain network are not yet clearly defined at the macroscopic scale. Previous studies have used the parcellation method to compose nodes [2], [6], [7]. However, this method is somewhat problematic in that network structures are influenced by changes in both the parcellation scale and the thresholding connectivity matrix. To overcome these problems, we proposed a novel brain network construction technique called as the ε-neighbor construction method. We examined structural characteristics of the brain networks using the proposed method and compared these characteristics against the parcellation method. We also examined how connectedness changes according to the parcellation scale or ε–radius. Because some nodes remained disconnected from the largest connected component, connectedness decreased when the parcellation method was used and the parcellation scale became finer, as shown in Fig. 12. The clustering coefficient and path lengths of disconnected nodes from the largest connected component were generally set to 0 and infinity, respectively, and these nodes were excluded when computing average clustering coefficients and path lengths for more robust computation. Due to the increase in number of disconnected nodes, topological properties such as clustering coefficient, average path length, and small-worldness do not meaningfully characterize network structures [51].

In the parcellation method, the connectedness from networks excluded nodes that tract endpoints do not reside into was close to 1 and the number of nodes decreased. The parcellation method excluded empty nodes would be a new approach and left as a future study. Tracts were considered unusable if endpoints did not belong to one of the parcellations in the AAL template, approximately 30% of them were unusable in the parcellation method. However, all tracts were considered usable in the proposed method. Our proposed method may have an additional advantage.

In networks constructed by the proposed method, connectedness did not change with scale (ε-radius). Thus, for any ε-radius, the topological properties of network can be characterized in a meaningfully manner. To compare the parcellation method with the proposed method, we examined topological properties for two chosen scales (i.e., 116 and 221 nodes) between control subjects and subjects with autism. Furthermore, we found more significant differences in the characteristics of brain networks of autistic versus non-autistic subjects when these networks were constructed using the proposed method than when the conventional parcellation method was used.

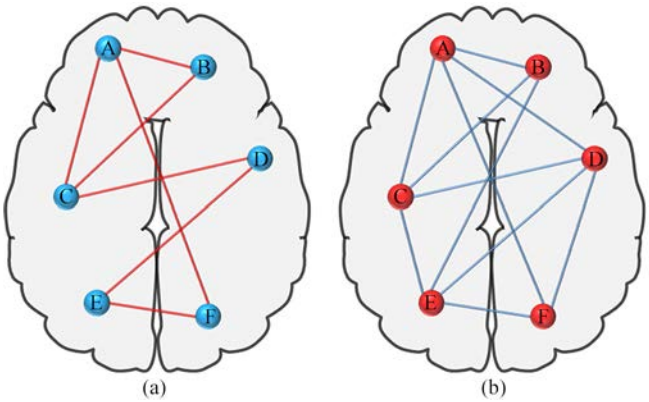

Fig. 13. Schematic diagraph of brain networks. (a) Typical connectivity in a control subject. (b) Typical overconnectivity in a subject with autism. Subjects with autism had brain networks with shorter path length, higher global efficiency, higher density, and higher node degree than those of control subjects.

Autism is widely known abnormalities in several areas of the brain, including the frontal lobe, the mirror neuron system, the limbic system, the temporal lobe, and the corpus callosum. Many recent studies have analyzed subjects with autism using techniques such as fMRI and DTI [12], [17]. These studies have tested the pervading hypothesis that brain connectivity in subjects with autism is abnormal. Here, we addressed this important issue by analyzing and comparing structural brain networks from control subjects and subjects with autism using the ε-neighbor construction method that does not use parcellation scheme. We analyzed the brain networks constructed by this method by comparing global topological characteristics between the two groups. We observed significant differences between networks constructed from control subjects and subjects with autism with respect to path length, E_{glob}, node degree, and density. More randomly connected networks tend to have shorter path lengths and higher E_{glob} [52] than more structured networks, which may reflect less organization in the former [9], [18]. From the results of global properties which had a shorter average path length, higher E_{glob}, higher density, and higher degree in subjects with autism, we concluded that subjects with autism exhibited overconnected brain network. Presence of structural connections between any two regions of brain can imply strong functional connections between them [53]. Thus, overconnected structural brain nework may be closely related with functional overconnectivity. More recent study suggests that subjects with autism showed functionally whole brain overconnectivity and it is related to impairments in the social domain [54]. This overconnectivity could cause the increase of synaptic excitation and decrease of synaptic inhibition. Imbalance of synaptic reaction could lead to functional deficits observed in autism [54]. Fig. 13 shows an example of overconnected brain network in autism.

In addition, we examined the structural characteristics of the brain networks of subjects with autism for targeted node attack based on NBC. In this analysis, we observed significant differences between two groups in the size of the largest connected components. More tolerant network for targeted node attack indicates that the network has more potential alternative paths [27]. This result indicated that subjects with autism had more overconnected nodes. Because of this, the subjects with autism steadily preserved the size of the largest connected component compared to control subjects for targeted node attack. The analysis of targeted node attack also suggests that brain network of subjects with autism is overconnected.

To identify regional abnormality caused by the structural overconnectivity in subjects with autism, we analyzed property of the regional level in the brain network using E_{reg}. In comparisons of E_{reg}, subjects with autism had increased E_{reg} in the right superior temporal gyrus and the left middle temporal gyrus than control subjects. These affected regions are consistent with those reported in prior studies based on fMRI, electroencephalogram (EEG), and DTI data [55]-[59]. Temporal gyrus is critical pathways involved in language and social cognition. Abnormalities of this region may be causative of the neurobehavioral features observed in autism [58]. Especially, superior temporal gyrus is connected to regions of association and limbic system [60] and may be crucial in face and gaze processing [61] and is related to emotional responses which also related to social cognition including visual, auditory and olfactory [62].

There is a need to simulate a ground truth signal for our proposed method. However, there are too many different possibilities of simulating a ground truth with the streamline based tractography. In addition, the simulation needs to generate many different types of ground truths and evaluate the degree of accuracy with which this difference can be detected. This issue is beyond the scope of the current paper, further study is needed to advance the results found here. Even though there is a limitation, we at least attempted to simulate the null data between two groups through the split-half experiment.

XI. Conclusion

Using our proposed method, network connectedness remained at a high level even as the number of nodes increased, indicating that our method is more realistic than the parcellation method. The brain networks constructed using our proposed method were small-world networks that had an exponentially truncated power law distribution consistent with previous human brain network studies. Based on our constructed networks, we found the evidence of global and regional abnormalities in subjects with autism. Our proposed method may provide new insights to analysis in the structural brain network. In a future study, we intend to apply our method to more subjects to further validate our results and various psychiatric and neurological disorders.

Acknowledgment

We would like to thank Kim M. Dalton and Nagesh Adluru of Waisman Center at the University of Wisconsin-Madison, and S.-G. Kim of Max Planck Institute, Germany for valuable discussions and image preprocessing supports.

REFERENCES

[1] O. Sporns et al., "Organization, development and function of complex brain networks," Trends Cogn. Sci., vol. 8, no. 9, pp. 418-425, 2004.

[2] G. Gong et al., "Mapping anatomical connectivity patterns of human cerebral cortex using in vivo diffusion tensor imaging tractography," Cereb. Cortex, vol. 19, no. 13, pp. 524-536, 2009.

[3] O. Sporns et al., "The human connectome: A structural description of the human brain," PLoS Comput. Biol., vol. 1, no. 4, pp. e42, 2005.

[4] M. Rubinov and O. Sporns, "Complex network measures of brain connectivity: Uses and interpretations," Neuroimage, vol. 52, no. 3, pp. 1059-1069, 2010.

[5] M. A. Just et al., "Functional and anatomical cortical underconnectivity in autism: Evidence from an fMRI study of an executive function task and corpus callosum morphometry," Cereb. Cortex, vol. 17, no. 4, pp. 951-961, 2007.

[6] A. Zalesky et al., "Whole-brain anatomical networks: Does the choice of nodes matter?," Neuroimage, vol. 50, no. 3, pp. 970-983, 2010.

[7] Q. Cao et al., "Probabilistic diffusion tractography and graph theory analysis reveal abnormal white matter structural connectivity networks in drug-naive boys with attention deficit/hyperactivity disorder," J. Neurosci., vol. 33, no. 26, pp. 10676-10687, 2013.

[8] M. K. Chung et al., "Scalable Brain Network Construction on White Matter Fibers," in Proc. SPIE, vol. 7962, 2011, pp. 79624G.

[9] E. L. Dennis et al., "Altered structural brain connectivity in healthy carriers of the autism risk gene, CNTNAP2," Brain Connect., vol. 1, no. 6, pp. 447-459, 2011.

[10] American Psychiatric Association, Diagnostic and statistical manual of mental disorders, Washington, DC, USA, 1994.

[11] R. K. Kana et al., "Brain connectivity in autism," Front. Hum. Neurosci., vol. 8, pp. 349, 2014.

[12] M. K. Belmonte et al., "Autism and Abnormal Development of Brain Connectivity," J. Neurosci., vol. 24, no. 42, pp. 9228-9231, 2004.

[13] V. L. Cherkassky et al., "Functional connectivity in a baseline resting-state network in autism," Neuroreport, vol. 17, no. 16, pp. 1687-1690, 2006.

[14] N. M. Kleinhans et al., "Abnormal function connectivity in autism spectrum disorders during face processing," Brain, vol. 131, pp. 1000-1012, 2008.

[15] R. A. Müller et al., "Underconnected, but how? A survey of functional connectivity MRI studies in autism spectrum disorders," Cereb. Cortex, vol. 21, no. 10, pp. 2233-2243, 2011.

[16] N. Adluru et al., "Characterizing brain connectivity using ε-radial nodes: Application to autism classification," presented at the MICCAI Workshop Comput. Diffusion MRI, Beijing, China, 2010.

[17] M. K. Chung et al., "Characterization of Structural Connectivity in Autism using Graph Networks with DTI," presented at 16th Annu. Meeting Org. Hum. Brain Mapp., Barcelona, Spain, Jun 6-10, 2010.

[18] J. D. Rudie et al., "Altered functional and structural brain network organization in autism," Neuroimage-Clin., vol. 2, no. 1, pp. 79-94, 2013.

[19] N. Tzourio-Mazoyer et al., "Automated anatomical labeling of activations in SPM using a macroscopic anatomical parcellation of the MNI MRI single-subject brain," Neuroimage, vol. 15, no. 1, pp. 273-289, 2002.

[20] P. Hagmann et al., "Mapping the structural core of human cerebral cortex," PLoS. Biol., vol. 6, no. 7, pp. e159, 2008.

[21] J. Leskovec and E. Horvitz, "Planetary-Scale Views on an Instant-Messaging Network," in Proc. 17th Int. World Wide Web Conf., 2008, pp. 915-924.

[22] D. J. Watts and S. H. Strogatz, "Collective dynamics of 'small-world' networks," Nature, vol. 393, pp. 440-442, 1998.

[23] P. Hagmann et al., "Mapping human whole-brain structural networks with diffusion MRI," PLoS One, vol. 2, no. 7, pp. e597, 2007.

[24] V. Latora and M. Marchiori, "Efficient behavior of small-world networks," Phys. Rev. Lett., vol. 87, no. 19, pp. 198701, 2001.

[25] A. J. Lawrence et al., "Structural network efficiency is associated with cognitive impairment in small-vessel disease," Neurology, vol. 83, no. 4, pp. 304-311, 2014.

[26] E. T. Bullmore and D. S. Bassett, "Brain graphs: graphical models of the human brain connectome," Annu. Rev. Clin. Psycho., vol. 7, pp. 113-140, 2011.

[27] B. C. Bernhardt et al., "Graph-theoretical analysis reveals disrupted small-world organization of cortical thickness correlation networks in temporal lobe epilepsy," Cereb. Cortex, vol. 21, no. 9, pp. 2147-2157, 2011.

[28] P. Holme et al., "Attack vulnerability of complex networks," Phys. Rev. E, vol. 65, no. 5, pp. 056109, 2002.

[29] V. M. Eguíluz et al., "Scale-free brain functional networks," Phys. Rev. Lett., vol. 94, no. 1, pp. 018102, 2005.

[30] M. Kaiser, "A tutorial in connectome analysis: Topological and spatial features of brain networks," Neuroimage, vol. 57, no. 3, pp. 892-907, 2011.

[31] T. F. Coleman and J. J. Moré, "Estimation of Sparse Jacobian Matrices and Graph Coloring Problems," SIAM J. Numer. Anal., vol. 20, no. 1, pp. 187-209, 1983.

[32] A. Pothen and C. J. Fan, "Computing the Block Triangular Form of a Sparse Matrix," ACM Trans. Math. Softw., vol. 16, no. 4, pp. 303-324, 1990.

[33] T. H. Hsieh et al., "Diagnosis of Schizophrenia Patients Based on Brain Network Complexity Analysis of Resting-State fMRI," in Proc. 15th Int. Conf. Biomed. Eng., 2014, pp. 203-206.

[34] A. Fornito et al., "Network scaling effects in graph analytic studies of human resting-state fMRI data," Front. Syst. Neurosci., vol. 4, pp. 22, 2010.

[35] J. M. Anthonisse, "The rush in a directed graph," Stichting Mathematisch Centrum, Amsterdam, Netherlands, Tech. Rep. BN 9/71, 1971.

[36] L. C. Freeman, "A set of measures of centrality based on betweenness," Sociometry, vol. 40, no. 1, pp. 35-41, 1977.

[37] T. E. Nichols and A. P. Holmes, "Nonparametric permutation tests for functional neuroimaging: A primer with examples," Hum. Brain Mapp., vol. 15, no. 1, pp. 1-25, 2001.

[38] D. Fein, "The neuropsychology of autism," New York: Oxford University Press, 2011, ch. 3, pp. 51-52.

[39] A. Yandiki et al., "Spurious group differences due to head motion in a diffusion MRI study," Neuroimage, vol. 88, pp. 79-90, 2014.

[40] R. P. Woods et al., "Automated image registration: I. General methods and intrasubject, intramodality validation," J. Comput. Assist. Tomo., vol. 22, no. 1, pp. 139-152, 1998.

[41] P. Jezzard and R. S. Balaban, "Correction for geometric distortion in echo planar images from B0 field variations," Magn. Reson. Med., vol. 34, no. 1, pp. 65-73, 1995.

[42] D. C. Alexander and G. J. Barker, "Optimal imaging parameters for fiber-orientation estimation in diffusion MRI," Neuroimage, vol. 27, no. 2, pp. 357-367, 2005.

[43] H. Zhang et al., "High-dimensional spatial normalization of diffusion tensor images improves the detection of white matter differences: An example study using amyotrophic lateral sclerosis," IEEE. Trans. Med. Imaging, vol. 26, no. 11, pp. 1585-1597, 2007.

[44] P. A. Cook et al., "Camino: Open-source diffusion-MRI reconstruction and processing," in Proc. 14th Sci. Meeting Int. Soc. Magn. Reson. Med., 2006, pp. 2759.

[45] M. Lazar et al., "White matter tractography using diffusion tensor deflection," Hum. Brain Mapp., vol. 18, no. 4, pp. 306-321, 2003.

[46] A. Gruslys et al., "3000 non-rigid medical image registrations overnight on a single PC," in Proc. IEEE Nucl. Sci. Symp. Med. Imaging Conf., 2011, pp. 3073-3080.

[47] L. A. N. Amaral et al., "Classes of small-world networks," Proc. Nat. Acad. Sci., vol. 97, pp. 11149-11152, 2000.

[48] S. R. Kesler et al., "Brain network alterations and vulnerability to simulated neurodegeneration in breast cancer," Neurobiol. Aging, vol. 36, no. 8, pp. 2429-2442, 2015.

[49] E. D. Fagerholm et al., "Disconnection of network hubs and cognitive impairment after traumatic brain injury," Brain, vol. 138, no. Pt6, pp. 1696-1709, 2015.

[50] J. Qin et al., "Altered anatomical patterns of depression in relation to antidepressant treatment: Evidence from a pattern recognition analysis on the topological organization of brain networks," J. Affect. Disord., vol. 180, pp. 129-137, 2015.

[51] K. Supekar et al., "Network analysis of intrinsic functional brain connectivity in Alzheimer's disease," PLoS Comput. Biol., vol. 4, no. 6, pp. e1000100, 2008.

[52] E. Bullmore and O. Sporns, "Complex brain networks: graph theoretical analysis of structural and functional systems," Nat. Rev. Neurosci., vol. 10, no. 3, pp. 186-198, 2009.

[53] Z. Wang et al., "The relationship of anatomical and functional connectivity to resting-state connectivity in primate somatosensory cortex," Neuron, vol. 78, no. 6, pp. 1116-1126, 2013.

[54] K. Supekar et al., "Brain hyperconnectivity in children with autism and its links to social deficits," Cell Reports, vol. 5, no. 3, pp. 738-747, 2013.

[55] N. Barnea-Goraly et al., “White matter structure in autism: preliminary evidence from diffusion tensor imaging,” Biol. Psychiatry, vol. 55, no. 3, pp. 323-326, 2004.
[56] G. Dawson et al., “Subgroups of autistic children based on social behavior display distinct patterns of brain activity,” J. Abnorm. Child Psychol., vol. 23, no. 5, pp. 569-583, 1995.
[57] P. G. Enticott et al., “Electrophysiological signs of supplementary-motor-area deficits in high-functioning autism but not Asperger syndrome: an examination of internally cued movement-related potentials,” Dev. Med. Child Neurol., vol. 51, no. 10, pp. 787-791, 2009.
[58] J. E. Lee et al., “Diffusion tensor imaging of white matter in the superior temporal gyrus and temporal stem in autism,” Neurosci. Lett., vol. 424, no. 2, pp. 127-132, 2007.
[59] J. G. Levitt et al., “Cortical sulcal maps in autism,” Cereb. Cortex, vol. 13, no. 7, pp. 728-735, 2003.
[60] R. J. Jou et al., “Enlarged right superior temporal gyrus in children and adolescents with autism,” Brain Res., vol. 1360, pp. 205-212, 2010.
[61] A. Puce et al., “Temporal cortex activation in humans viewing eye and mouth movements,” J. Neurosci., vol. 18, no. 6, pp. 2188-2199, 1998.
[62] J. P. Royet et al., “Emotional responses to pleasant and unpleasant olfactory, visual, and auditory stimuli: A positron emission tomography study,” J. Neurosci., vol. 20, no. 20, pp. 7752-7759, 2000.